A theoretical study of the annual variation of atmospheric energy[1]

By A. WIIN-NIELSEN, *Department of Meteorology and Oceanography, The University of Michigan, Ann Arbor, Michigan*

(Manuscript received, May 5, 1969)

ABSTRACT

The zonally averaged equation for a two-level, quasi-geostrophic model are used to calculate the annual mean values and the first harmonic of the annual variation of the midtropospheric temperature and the zonal winds at the upper and lower levels. The diabatic heating in the model is of a simple Newtonian form. The effects of surface skin friction and of internal friction are included together with a simple parameterization of the meridional eddy transport of sensible heat, while the transport of zonal relative momentum by the eddies is neglected, thereby restricting the motion to the largest meridional scale. From the solution of the equations it is possible to calculate the annual mean values and the first harmonic of the annual variation of the amounts of zonal available potential energy and zonal kinetic energy and, also, the generation of zonal available potential energy, the convertions from this form of energy to eddy available potential energy and to zonal kinetic energy, and the dissipation of zonal kinetic energy by friction.

The results show that the simplified model is capable of reproducing several important aspects of the annual variation of atmospheric energetics. The phase relationships involving the time lag between the generation of zonal available potential energy and the dissipation of kinetic energy as well as the time lag between the seasonal forcing and the maxima of zonal available potential energy and zonal kinetic energy are well reproduced. There are differences between the theoretical results and observational studies with respect to the intensity of the general circulation and the amounts of energy.

The sensitivity of the theoretical solution to the numerical values of the physical parameters is investigated.

1. Introduction

In a recent paper (Wiin-Nielsen, 1968) the author described a preliminary study of the atmospheric response to large scale seasonal forcing. Diagnostic studies of the energetics of the large scale motion in the atmosphere (Krueger *et al.*, 1965; Wiin-Nielsen, 1967; Kung & Soong, 1969) have shown that there exists a typical time lag between the maximum generation of available potential energy and the dissipation of kinetic energy. The time lag is of the order of magnitude of one month. These studies have also shown that the available potential energy and the kinetic energy have maxima in late January approximately one month after the winter solstice.

The preliminary study (Wiin-Nielsen, 1968) attempted to give a theoretical explanation of the results obtained in the observational studies by considering solutions of the zonally averaged equations for the quasi-geostrophic, two-level model including Newtonian heating and frictional dissipation. However, the solution was based on Cartesian geometry and the Newtonian heating as well as the dependent variables were approximated by a single sinusoidal component satisfying the necessary boundary conditions at walls to the south and the north. Although such approximations greatly simplify the problem, they are unrealistic in several respects, and it is one of the purposes of this paper to remove these simplifications.

Another approximation of the preliminary study was the neglect of the meridional transport of zonal relative momentum in comparison with other processes included in the model. It was shown that this approximation is well justified

[1] Research supported by the National Science Foundation, GA-841. Contribution No. 150, Department of Meteorology and Oceanograhpy, The University of Michigan, Ann Arbor.

if the south–north scale of the motion is of the same order of magnitude as the distance between equator and pole, but that the effect of the momentum transport becomes less justified the smaller the south–north scale is. It is realized that this approximation must be removed when a good parameterization of the momentum transport has been found. The results of a recent study of Saltzman & Vernekar (1968) cannot be applied here, because they assume that seasonal variations have been removed from the motion. Another idea dealing with the parameterization of the momentum transport has been expressed by Green (1968). This approach assumes that a diffusion approximation can be made for the transport of the quasi-conservative quantities of entropy and potential vorticity. The divergence of the momentum transport can then be calculated indirectly. The applicability of this idea is presently under investigation, and the results will be described in a separate paper to be published in the near future. However, for this study we shall neglect the horizontal momentum transport and restrict ourselves to the largest meridional scale of motion. The implications of this assumption are naturally that we cannot expect to account for all the details in the profiles of the temperature and the wind, but since we are mainly interested in the annual variation of the energetics of the atmosphere, we may not need all the details.

2. The atmospheric model

The earlier paper (Wiin-Nielsen, 1968) contains a description of the details of the atmospheric model including a description of the energy sources and sinks incorporated in the study. The paper contains also an analysis of the order of magnitude of various terms including the justification of the neglect of the meridional transport of zonal relative momentum. In this paper it will therefore be sufficient to reproduce the simplified equations which are to be solved. They are:

$$\frac{\partial \zeta_*}{\partial t} = -\varepsilon\zeta_* + 2\varepsilon\zeta_T, \tag{2.1}$$

$$\frac{\partial}{\partial t}(\zeta_T - q^2\bar{\psi}_T) = \varepsilon\zeta_{*T} - [2(\varepsilon + A) + q^2K]\zeta_T + q^2\gamma(\bar{\psi}_T - \bar{\psi}_E). \tag{2.2}$$

In these equations, ψ is the stream function and $\zeta = \nabla^2\psi$ the relative vorticity. An asterisk as a subscript is defined as half the sum of the quantity at the upper level (subscript 1) and at the lower level (subscript 3), i.e.,

$$(\ )_* = \frac{1}{2}[(\ )_1 + (\ )_3] \tag{2.3}$$

while the subscript T is defined as half the difference between these quantities, i.e.,

$$(\ )_T = \frac{1}{2}[(\ )_1 - (\ )_3]. \tag{2.4}$$

A bar over a quantity denotes a zonal average, i.e.,

$$\overline{(\ )} = \frac{1}{2\pi}\int_0^{2\pi} (\ )\,d\lambda, \tag{2.5}$$

where λ is longitude.

The equations contain five parameters, q, ε, A, γ, and K. They are defined in the following way. The quantity, q, is the usual measure of static stability appearing in a two-level, quasi-geostrophic model:

$$q^2 = \frac{2f_0^2}{\sigma_2 P^2}, \tag{2.6}$$

where f_0 is a standard value of the Coriolis parameter, $P = 50$ cb, and $\sigma = -\alpha\partial \ln \theta/\partial p$. In the last expression α is the specific volume, θ the potential temperature, and p pressure.

The quantity ε is a measure of the intensity of the surface skin friction. It is defined by the expression

$$\varepsilon = \frac{gC_d\,\varrho_4\,V_4}{2P}, \tag{2.7}$$

where g is the acceleration of gravity, C_d the drag coefficient, ϱ_4 a standard value of the surface density, and V_4 a typical value of the windspeed at the surface.

A is a measure of the intensity of the internal friction in the atmosphere. The numerical value of A is computed from the expression:

$$A = \frac{g^2\nu}{R^2\tilde{T}_2^2}, \tag{2.8}$$

where ν is the coefficient of eddy viscosity, R the gas constant, and $\tilde{T}_2$ a typical value of the temperature at 50 cb.

γ is a measure of the intensity of the diabatic heating in the model. The heating is of Newtonian form:

$$H_2 = -\gamma C_p(T_2 - T_E), \tag{2.9}$$

where H_2 is the heating per unit mass and unit time, C_p the specific heat for constant pressure, T_2 the temperature at 50 cb, and T_E the equilibrium temperature at the same level, while γ is a proportionality factor.

Finally, K is the diffusion coefficient for the meridional transport of sensible heat. K is defined through the equation

$$\overline{T_* v_*} = -K \frac{\partial \overline{T}_*}{a \partial \varphi}, \tag{2.10}$$

where v is the meridional component of the wind, a the radius of the earth, and φ is latitude. The assumption (2.10) is reasonably good because we are dealing with the vertical average of the transport of sensible heat in a two-level model. The approximation could not be used with any accuracy in the lower layers of the stratosphere, where the temperature gradient is reversed while the heat transport still is from south to north. In this study we shall assume that K is a constant, but it is realized that K will vary with latitude, pressure, and time. A calculation which will describe these variations of K as obtained from meteorological data is presently underway, and the results will be given in a separate paper in the near future.

3. The equilibrium temperature

In order to integrate eqs. (2.1) and (2.2) it is necessary to specify the dependence of $\bar{\psi}_E$ on latitude and time. We note first of all that the thermal equilibrium stream function ψ_E is related to the temperature T_E through the formula:

$$\psi_E = \frac{R}{2f_0} T_E \tag{3.1}$$

obtained through the use of the gas equation and the hydrostatic relation. Although T_E formally applies at level 2 (50 cb), we shall interpret T_E as an equilibrium temperature for a vertical column in the atmosphere. It is now possible to calculate T_E using the method given by Saltzman (1968). In this study, we restrict ourselves to a consideration of the short- and long-wave radiation and neglect the effects of small-scale convection, evaporation, and condensation as well as the subsurface conduction and convection. The equilibrium equations for the atmosphere (50 cb) and the surface of the earth are then, respectively:

$$\chi(1 - r_a)R_0 + \Gamma\sigma T_{SE}^4 - (\nu_1 + \nu_2)\sigma T_E^4 = 0, \tag{3.2}$$

$$(1 - \chi)(1 - r_a)(1 - r_s)R_0 + \nu_1 \sigma T_E^4 - \sigma T_{SE}^4 = 0 \tag{3.3}$$

The symbols in (3.2) and (3.3) are defined in the list given below. Some symbols, such as ν and σ, were also used in section 2 of this paper. In order to avoid any misunderstanding it should be stressed that eqs. (3.2) and (3.3) are used for the single purpose of calculating the equilibrium temperature field $T_E = T_E(\varphi, t)$ as a separate calculation made once and for all.

The list of symbols is:

- χ = opacity of the atmosphere to solar radiation
- r_s = albedo of the surface
- r_a = albedo of the atmosphere
- Γ = long-wave absorptivity of the atmosphere
- ν_1, ν_2 = factors for downward and upward effective black-body long-wave radiation from the atmosphere, respectively
- σ = Stefan-Boltzman constant
- R_0 = intensity of the solar radiation at the top of the atmosphere
- T_E = equilibrium temperature (50 cb)
- T_{SE} = surface equilibrium temperature

It is seen that eqs. (3.2) and (3.3) can be considered as two equations with the unknown T_E and T_{SE}, if we can give the numerical values of χ, r_s, r_a, Γ, ν_1, ν_2, and σ, and if R_0 is known as a function of latitude and time. In this calculation we have adopted the values given by Saltzman (1968) for the constants and the values of R_0 were taken from the Smithsonian Meteorological Tables (1951). After we have solved for T_E^4 from (3.2) and (3.3), we have adopted the approximation

$$T^4 = 4T_0^3 T - 3T_0^4, \quad T_0 = 273° \text{ K}. \tag{3.4}$$

It is then possible to write $\overline{T}_E$ in the form

$$\overline{T}_E = aR_0 + b, \tag{3.5}$$

Table 1. *The zonally averaged equilibrium temperatures as a function of latitude and time*

	Jan.	Feb.	Mar.	Apr.	May	June	July	Aug.	Sept.	Oct.	Nov.	Dec.
90	204.75	204.75	204.75	236.75	264.98	278.56	274.33	251.01	214.99	204.75	204.75	204.75
80	204.75	204.99	213.01	236.48	264.07	277.41	273.35	250.47	221.96	205.65	204.75	204.75
70	204.90	210.17	223.16	242.91	262.37	274.11	270.13	252.01	231.25	214.27	205.89	204.75
60	210.32	219.52	233.05	250.30	264.80	272.37	269.78	257.21	240.27	224.34	213.31	208.70
50	219.63	229.53	242.27	256.84	267.92	273.35	271.53	262.07	248.36	234.16	222.94	217.70
40	229.78	239.29	250.45	261.89	270.14	273.73	272.44	265.66	255.11	243.27	232.97	227.63
30	239.80	248.08	257.17	265.71	270.82	272.84	271.95	267.85	260.53	251.45	242.62	237.95
20	249.23	255.85	262.36	267.51	269.69	270.20	269.85	268.20	264.22	258.15	251.40	247.59
10	257.66	262.15	265.85	267.51	266.93	266.02	266.14	266.79	266.11	263.30	259.06	256.40
0	264.75	266.84	267.42	265.64	262.44	260.34	260.75	263.54	266.16	266.77	265.22	263.94
−10	270.27	269.74	267.18	262.02	256.50	253.25	254.03	258.74	264.33	268.34	269.73	270.02
−20	274.11	270.76	264.97	256.68	249.12	244.96	246.05	252.36	260.71	268.03	272.53	274.43
−30	276.17	269.88	260.98	249.83	240.63	235.84	237.16	244.68	255.39	265.82	273.48	277.15
−40	276.49	267.08	255.25	241.63	231.36	226.19	227.71	236.00	248.61	261.68	272.69	278.17
−50	275.35	262.88	248.10	232.48	221.80	216.87	218.19	226.66	240.49	256.27	270.35	277.73
−60	273.28	257.21	239.63	222.77	212.58	208.47	209.51	217.15	231.38	249.26	266,84	276.65
−70	273.27	251.09	230.30	212.98	205.73	204.75	204.75	208.52	221.63	241.35	264.03	278.48
−80	276.39	247.80	220.49	205.20	204.75	204.75	204.75	204.90	211.88	234.01	265.67	281.95
−90	277.49	248.25	212.34	204.75	204.75	204.75	204.75	204.75	204.75	233.58	266.53	283.09

where $a = 0.07$ and $b = 204.75°$K, when R_0 is given in the units of the table (cal cm^{-2} day^{-1}). It should finally be noticed that the values given in the table were used to interpolate to new values which gave R_0 in the middle of each month of the year in order to facilitate the later calculations. The results of the calculations are presented in Table 1 of this paper giving T_E as a function of latitude and month in °K. The expression (3.1) was used to convert the values of T_E to $\bar{\psi}_E$ which form the input for the later calculations.

4. Method of solution

The model eqs. (2.1) and (2.2) are to be solved for the quantities $\bar{\psi}_*$ and $\bar{\psi}_T$ considering $\bar{\psi}_E$ as known. In this study we are mainly interested in the annual mean values and in the first harmonic of the annual variation which has a much larger amplitude than any of the higher harmonics in the energy quantities which have been analyzed in observational studies (Wiin-Nielsen, 1967). In view of the nature of the equations, it is natural to seek solutions to the equations by expanding each of the dependent variables in a series of Legendre functions. Consequently, we write:

$$\bar{\psi}_E = \sum_{n=0}^{N} (\tilde{E}_n + E'_n(t))\, P_n(\varphi), \qquad (4.1)$$

$$\bar{\psi}_T = \sum_{n=0}^{N} (\tilde{T}_n + T'_n(t))\, P_n(\varphi) \qquad (4.2)$$

and

$$\bar{\psi}_* = \sum_{n=0}^{N} (\tilde{S}_n + S'_n(t))\, P_n(\varphi), \qquad (4.3)$$

where $P_n(\varphi)$ is the Legendre polynomial of the first kind and of the nth degree. The Legendre coefficients have been written as a sum of the annual mean value, denoted by a tilde, and the deviation from this mean. In view of the fact that we shall restrict ourselves to the first harmonic of the annual variation we write:

$$E'_n(t) = A_n^E \cos st + B_n^E \sin st, \qquad (4.4)$$

$$T'_n(t) = A_n^T \cos st + B_n^T \sin st, \qquad (4.5)$$

$$S'_n(t) = A_n^S \cos st + B_n^S \sin st, \qquad (4.6)$$

where s is the frequency corresponding to the period of one year, i.e., $s = 0.2 \times 10^{-6}$ sec.$^{-1}$

We note that the relative vorticity is given by the formula

$$\zeta = -\frac{1}{a\cos\varphi}\frac{\partial \bar{u}\cos\varphi}{\partial\varphi} = \frac{1}{a^2\cos\varphi}\frac{\partial}{\partial\varphi}\left[\cos\varphi\frac{\partial\bar{\psi}}{\partial\varphi}\right]$$

$$= \frac{1}{a^2}\frac{\partial}{\partial\mu}\left[(1-\mu^2)\frac{\partial\bar{\psi}}{\partial\mu}\right], \qquad (4.7)$$

where

$$\mu = \sin\varphi. \qquad (4.8)$$

Substituting from anyone of the expressions (4.1)–(4.3), say (4.2), we get:

$$\zeta_T = \sum_{n=0}^{N} (\tilde{T}_n + T'_n(t)) \frac{1}{a^2} \frac{d}{d\mu} \left[(1-\mu^2) \frac{dP_n}{d\mu} \right] \quad (4.9)$$

but $P_n = P_n(\mu)$ satisfies the equation

$$\frac{d}{d\mu} \left[(1-\mu^2) \frac{dP_n}{d\mu} \right] + n(n+1)P_n = 0. \quad (4.10)$$

We have therefore

$$\zeta_T = -\sum_{n=0}^{N} (\tilde{T}_n + T'_n(t)) \frac{n(n+1)}{a^2} P_n \quad (4.11)$$

and, in an analogous way:

$$\zeta_* = -\sum_{n=0}^{N} (\tilde{S}_n + S'_n(t)) \frac{n(n+1)}{a^2} P_n. \quad (4.12)$$

The series (4.1), (4.2), (4.11), and (4.12) are substituted in the basic equations, (2.1) and (2.2), for the model. Equating first the time-independent terms and solving for $\tilde{S}_n$ and $\tilde{T}_n$ in terms of $\tilde{E}_n$ we find:

$$\tilde{S}_n = 2\tilde{T}_n \quad (4.13)$$

and

$$\tilde{T}_n = \tilde{r}_n \tilde{E}_n, \quad (4.14)$$

where

$$\tilde{r}_n = \frac{\gamma q^2 a^2}{n(n+1)(2A + q^2K) + \gamma q^2 a^2}. \quad (4.15)$$

We noticed that $\tilde{r}_n = 1$, when $n = 0$, and that $\tilde{r}_n < 1$ for $n > 0$. It is thus obvious that the series involving the annual mean values in (4.2) and (4.3) will converge more rapidly than the corresponding series in (4.1).

Equating next the time-dependent terms in eqs. (2.1) and (2.2) we obtain after a slight rearrangement:

$$\frac{dS'_n}{dt} = -\varepsilon S'_n + 2\varepsilon T'_n \quad (4.16)$$

and

$$\left(1 + \frac{q^2 a^2}{n(n+1)}\right) \frac{dT'_n}{dt} = \varepsilon S_n - [2(\varepsilon + A) + q^2 K] T'_n - \frac{\gamma q^2 a^2}{n(n+1)} (T'_n - E'_n). \quad (4.17)$$

The expressions (4.4)–(4.6) may also be written in the form:

$$E'_n(t) = \mathrm{Re}\,[C^E_n e^{ist}], \quad C^E_n = A^E_n - iB^E_n, \quad (4.18)$$

$$T'_n(t) = \mathrm{Re}\,[C^T_n e^{ist}], \quad C^T_n = A^T_n - iB^T_n, \quad (4.19)$$

$$S'_n(t) = \mathrm{Re}\,[C^S_n e^{ist}], \quad C^S_n = A^S_n - iB^S_n. \quad (4.20)$$

Substituting first in (4.16) and solving for C^S_n we find:

$$C^S_n = \frac{2\varepsilon}{\varepsilon^2 + s^2} (\varepsilon - is)\, C^T_n. \quad (4.21)$$

The expression (4.21) is substituted in (4.17) together with the expressions (4.18)–(4.20). After some manipulations we find that the solution for C^T_n can be written in the form

$$C^T_n = \frac{d_n}{a_n + ib_n} C^E_n, \quad (4.22)$$

where

$$a_n = 2A + q^2 K + \frac{\gamma q^2 a^2}{n(n+1)}, \quad (4.23)$$

$$b_n = s\left(3 + \frac{q^2 a^2}{n(n+1)}\right), \quad (4.24)$$

$$d_n = \frac{\gamma q^2 a^2}{n(n+1)}. \quad (4.25)$$

The solution (4.22) applies for $n \neq 0$. For $n = 0$ we get:

$$C^T_0 = \frac{\gamma}{\gamma^2 + s^2} (\varepsilon - is)\, C^E_0. \quad (4.26)$$

The development given above constitutes the formal solution of the problem. The major steps in the calculations necessary to obtain the solution are given below.

The starting point for the calculation is the data given in Table 1. Then equilibrium temperatures are converted to equilibrium stream functions $\bar{\psi}_E$ using eq. (3.1). The stream function $\bar{\psi}_E(\varphi, t)$ is given in the region $-\pi/2 \leqslant \varphi \leqslant +\pi/2$ for each 10° of latitude and with values applicable to each month. We shall denote these times by $t_1, t_2, \ldots, t_{12}$. The next step is to compute $E_n(t) = \tilde{E}_n + E'_n(t)$ for each of the values $t = t_K$. We have:

$$E_n(t_K) = \frac{2n+1}{2} \int_{-\pi/2}^{+\pi/2} \bar{\psi}_E(\varphi, t_K)\, P_n(\varphi) \cos\varphi\, d\varphi. \quad (4.27)$$

The integral (4.27) is evaluated as a finite sum using the approximation

$$E_n(t_K) = \frac{2n+1}{2} \cdot \Delta\varphi \sum_{j=1}^{17} \{\bar{\psi}_E(\varphi_j, t_K)\, P_n(\varphi_j) \cos\varphi_j\}, \tag{4.28}$$

where
$$\Delta\varphi = \frac{1}{18} \cdot \pi \tag{4.29}$$

and $\varphi_1 = -80°$, $\varphi_2 = -70°$, ..., $\varphi_{17} = +80°$.

The numerical values of $P_n(\varphi_j)$ can be generated in the following way. It is known that $P_0 = 1$ and $P_1 = \sin\varphi$. Starting from these values we can calculate P_n for $n \geq 2$ with the aid of the recurrence formula:

$$P_n = \frac{2n-1}{n} \sin\varphi\, P_{n-1} - \frac{n-1}{n} P_{n-2}. \tag{4.30}$$

When the values of $E_n(t_K)$ have been computed we proceed to calculate the values of $\tilde{E}_n$ and A_n^E and B_n^E using the formulas:

$$\tilde{E}_n = \frac{1}{12} \sum_{K=1}^{12} E_n(t_K), \tag{4.31}$$

$$A_n^E = \frac{1}{6} \sum_{K=1}^{12} \left\{ E_n(t_K) \cos\left[\frac{\pi}{12} + \frac{\pi}{6}(K-1)\right]\right\}, \tag{4.32}$$

$$B_n^E = \frac{1}{6} \sum_{K=1}^{12} \left\{ E_n(t_K) \sin\left[\frac{\pi}{12} + \frac{\pi}{6}(K-1)\right]\right\}. \tag{4.33}$$

The values of $\tilde{S}_n$ and $\tilde{T}_n$ are then obtained from (4.13) and (4.14) using the expression (4.15) for $\tilde{r}_n$, while C_n^S and C_n^T are calculated from (4.21) and (4.22), respectively, using (4.23)–(4.25) for a_n, b_n, and d_n.

The annual mean values, $\tilde{\psi}_T$ and $\tilde{\psi}_*$, of ψ_T and ψ_* can now be computed from the truncated series:

$$\tilde{\psi}_T(\varphi_j) = \sum_{n=0}^{N} \tilde{T}_n\, P_n(\varphi_j) \tag{4.34}$$

and
$$\tilde{\psi}_*(\varphi_j) = \sum_{n=0}^{N} \tilde{S}_n\, P_n(\varphi_j). \tag{4.35}$$

The deviations from the annual mean as expressed by the first harmonic can be written in the form:

$$\psi_T'(\varphi_j) = G^T(\varphi_j) \cos st + H^T(\varphi_j) \sin st \tag{4.36}$$

and
$$\psi_*'(\varphi_j) = G^S(\varphi_j) \cos st + H^S(\varphi_j) \sin st, \tag{4.37}$$

where
$$G^T(\varphi_j) = \sum_{n=0}^{N} A_n^T P_n(\varphi_j), \tag{4.38}$$

$$H^T(\varphi_j) = \sum_{n=0}^{N} B_n^T P_n(\varphi_j), \tag{4.39}$$

$$G^S(\varphi_j) = \sum_{n=0}^{N} A_n^S P_n(\varphi_j), \tag{4.40}$$

$$H^S(\varphi_j) = \sum_{n=0}^{N} B_n^S P_n(\varphi_j). \tag{4.41}$$

It is seen from (4.36) and (4.37) that we may express the annual variation as an amplitude and a phase angle. This will be done later, and the phase will be computed as the time δ at which the annual variation is at its maximum, i.e.,

$$\delta = \frac{1}{s} \arctan\left(\frac{H}{G}\right). \tag{4.42}$$

5. Energy considerations

The procedure given in sections 2, 3, and 4 of this paper gives solutions for $\bar{\psi}_*$ and $\bar{\psi}_T$. It is naturally possible to derive a large number of quantities from the solution such as zonal wind and temperature distributions. It should also be pointed out that the zonally averaged vertical velocity $\bar{\omega}$ can be calculated from the thermodynamic equation.

One of the main purposes of this study is to consider the energetics of the calculations, because most of the observational studies have concentrated on the annual variation of various energy quantities (Wiin-Nielsen, 1967, and Kung & Soong, 1969). The energetics of the two-level, quasi-geostrophic model is well known and need not be repeated here. We note that we are restricted to consider the energy budgets of the zonal components, A_Z and K_Z, of the available potential and kinetic energies because of the parameterization of the transport processes. Furthermore, we shall find it advantageous to divide the kinetic energy into the energy of the vertically averaged flow, K_{Z*}, and the energy of the deviation from this flow K_{ZT} as described by Wiin-Nielsen (1962). With reference to this paper and to Phillips (1956) we state the following formulas for the amounts of energy:

$$A_Z = \frac{P}{g} q^2 \int_0^{\pi/2} \bar{\psi}_{T,d}^2 \cos\varphi \, d\varphi, \qquad (5.1)$$

$$K_{ZT} = \frac{P}{g} \int_0^{\pi/2} \bar{u}_T^2 \cos\varphi \, d\varphi, \qquad (5.2)$$

$$K_{Z*} = \frac{P}{g} \int_0^{\pi/2} \bar{u}_*^2 \cos\varphi \, d\varphi, \qquad (5.3)$$

where $\bar{u}_T = -a^{-1}\partial\bar{\psi}_T/\partial\varphi$ and $\bar{u}_* = a^{-1}\partial\bar{\psi}_*/\partial\varphi$. Also the subscript d indicates a deviation from the area mean.

Note, that the energy quantities are calculated over the Northern Hemisphere only. The reasons are that we have no observational studies from the Southern Hemisphere of these details of the energetics, and, more importantly, the energetics of the total globe will show a very small annual variation because the intense circulation in one of the hemispheres during winter will be compensated by a much weaker circulation in the summer hemisphere. Half a year later, the situation will be reversed.

The generation of zonal available potential energy takes the following form when we substitute our expression for the Newtonian heating:

$$G(A_Z) = 2\frac{P}{g} q^2 \gamma \int_0^{\pi/2} \bar{\psi}_{T,d}(\bar{\psi}_{E,d} - \bar{\psi}_{T,d}) \cos\varphi \, d\varphi. \qquad (5.4)$$

The energy conversion from A_Z to K_Z is:

$$C(A_Z, K_Z) = -\frac{2f_0}{g} \int_0^{\pi/2} \bar{\psi}_T \bar{\omega} \cos\varphi \, d\varphi \qquad (5.5)$$

while the conversion from A_Z to A_E can be written in the form

$$C(A_Z, A_E) = -2\frac{P}{g} q^2 K \int_0^{\pi/2} \bar{\psi}_T \zeta_T \cos\varphi \, d\varphi \qquad (5.6)$$

when we use our empirical expression (2.10) for the transport of sensible heat.

We shall finally give the formulas for the dissipation of the two forms of kinetic energy. It turns out that

$$D(K_{TZ}) = 2\frac{P}{g} \int_0^{\pi/2} \bar{\psi}_T(\varepsilon\zeta_* - 2(\varepsilon + A)\zeta_T) \cos\varphi \, d\varphi \qquad (5.7)$$

and that

$$D(K_{*Z}) = -2\frac{P}{g} \varepsilon \int_0^{\pi/2} \bar{\psi}_*(\zeta_* - 2\zeta_T) \cos\varphi \, d\varphi. \qquad (5.8)$$

All the integrals appearing in (5.1)–(5.8) are or can be divided into integrals of the form:

$$I(X, Y) = \int_0^{\pi/2} X(t)\, Y(t) \cos\varphi \, d\varphi. \qquad (5.9)$$

In this study $X(t)$ and $Y(t)$ have the form:

$$X(t) = \tilde{X} + A^X \cos st + B^X \sin st. \qquad (5.11)$$

Substituting (5.10) and (5.11) into (5.9) we can write (5.9) in the form:

$$I(X, Y) = \widetilde{I(X, Y)} + I_C \cos st + I_S \sin st, \qquad (5.12)$$

where $$\widetilde{I(X, Y)} = \int_0^{\pi/2} \left[\tilde{X}\tilde{Y} + \frac{1}{2}(A^X A^Y + B^X B^Y)\right] \cos\varphi \, d\varphi \qquad (5.13)$$

and $$I_C = \int_0^{\pi/2} [\tilde{X}A^Y + \tilde{Y}A^X] \cos\varphi \, d\varphi \qquad (5.14)$$

and $$I_S = \int_0^{\pi/2} [\tilde{X}B^Y + \tilde{Y}B^X] \cos\varphi \, d\varphi \qquad (5.15)$$

The formulas (5.12) to (5.15) were used to evaluate all of the energy integrals listed in (5.1) to (5.8). We note again from (5.12) that the annual variation of an energy integral can be expressed as an amplitude and a phase angle. Note also that only the annual mean value and the first harmonic of the annual variation have been included in (5.12) consistent with the earlier formulation of the problem.

6. Results

Any numerical solution of our problem requires a selection of values for the physical parameters ε, A, γ, K, and q. ε can be calculated from (2.7). A reasonable estimate of ε is obtained if we use $g = 9.8$ m sec^{-2}, $C_d = 3 \times 10^{-3}$, $\varrho_4 = 1.3 \times 10^{-3}$ and $V_4 = 10$ m sec^{-1}. The resulting value of ε is 4×10^{-6} sec^{-1}, but it is obvious that ε cannot be determined with great accuracy because of the uncertainty in C_d and V_4. The parameter A is defined in (2.8). Using $R = 287$ m^2 sec^{-2} deg^{-1}, $\tilde{T}_2 = 250$°K and $\nu = 32$ m^2 sec^{-1} we find $A = 0.6 \times 10^{-6}$ sec^{-1}. The value of ν corre-

Table 2. *Values of* $\tilde{r}_n$ *as a function of n, when* $\varepsilon = 4 \times 10^{-6}\,\mathrm{sec}^{-1}$, $A = 0.6 \times 10^{-6}\,\mathrm{sec}^{-1}$, $\gamma = 0.4 \times 10^{-6}\,\mathrm{sec}^{-1}$, $K = 2 \times 10^{6}\,\mathrm{m}^2\,\mathrm{sec}^{-1}$, *and* $q^2 = 4 \times 10^{-12}\,\mathrm{m}^{-2}$

n	0	1	2	3	4	5	6	7	8	9	10
$\tilde{r}_n$	1.00	0.78	0.54	0.37	0.26	0.19	0.14	0.11	0.09	0.07	0.06

sponds to Palmén's (1955) estimate of $\varrho v = 2.25 \times 10^{-2}\,\mathrm{tm}^{-1}\,\mathrm{sec}^{-1}$, but it is known that ϱv may be larger than this value. Riehl (1951) finds for example a value of $\varrho v = 5 \times 10^{-2}\,\mathrm{tm}^{-1}\,\mathrm{sec}^{-1}$ which would increase the estimate of A to $1.3 \times 10^{-6}\,\mathrm{sec}^{-1}$. γ has been estimated by Wiin-Nielsen, Vernekar, and Yang (1967) to have a value of $0.4 \times 10^{-6}\,\mathrm{sec}^{-1}$. We shall not here go into the method of estimation except to point out that there is as large an uncertainty in γ as in ε and A.

The numerical value of K, defined in (2.10), has been considered by Adem (1962) and Saltzman (1968). The first author determines the values of K which are necessary to accomplish the required heat transport provided the expression (2.10) is correct. He finds a seasonal variation of K with large values in winter and small or vanishing values in summer. In this investigation we shall consider the case where K is constant by assumption. The value derived from Adem's (1962) data is $2.5 \times 10^6\,\mathrm{m}^2\,\mathrm{sec}^{-1}$ for the annual average. Saltzman (1968) finds also that the value of K is somewhat larger in winter than in summer with an average of $1.9 \times 10^6\,\mathrm{m}^2\,\mathrm{sec}^{-1}$. Finally, the value of q^2 has been selected to be $4 \times 10^{-12}\,\mathrm{m}^{-2}$ corresponding to a value of $f_0 = 10^{-4}\,\mathrm{sec}^{-1}$, $\sigma = 2\,\mathrm{m}^4\,\mathrm{sec}^2\,\mathrm{t}^{-2}$ and $P = 50$ cb.

The description of the results will be given in detail for a case where $\varepsilon = 4 \times 10^{-6}\,\mathrm{sec}^{-1}$, $A = 0.6 \times 10^{-6}\,\mathrm{sec}^{-1}$, $\gamma = 0.4 \times 10^{-6}\,\mathrm{sec}^{-1}$, $K = 2.0 \times 10^6\,\mathrm{m}^2\,\mathrm{sec}^{-1}$, and $q^2 = 4 \times 10^{-12}\,\mathrm{m}^{-2}$, which we will consider as typical values. Later we shall consider how sensitive the solution is to some of the physical parameters. Most of the calculations were carried out with $N = 10$ which means that we consider Legendre polynomials up to and including the 10th degree. However, it is obvious that the largest values of n give only a very small contribution to the solution as can be seen from Table 2 which gives the values of $\tilde{r}_n$ as a function of n for this case.

Fig. 1 shows two curves. The solid curve is the annual mean of the equilibrium temperature, while the dashed curve is the temperature $\tilde{T}_2$ computed from the model. It is obvious that the model manages to reduce the temperature contrast between equator and pole. While the temperature differences between equator and pole is 36°K for the equilibrium temperature $\tilde{T}_E$, it is only 25°K for the temperature $\tilde{T}_2$. The curves are only reproduced for the Northern Hemisphere, because it turns out that $\tilde{T}_E$ and $\tilde{T}_2$ are almost symmetric around the equator.

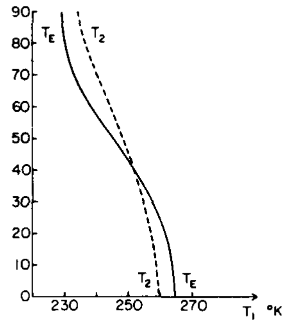

Fig. 1. The annual mean values of the equilibrium temperature $\tilde{T}_E$ and the computed temperature at 50 cb, $\tilde{T}_2$ as a function of latitude.

We consider next Fig. 2 which gives the temperature distributions at four times during the year: January 15, April 15, July 15, and October 15. In each of the four diagrams we have reproduced three curves: $T_E(\varphi)$, $T_2(\varphi)$ as computed from the model and an estimate of the observed temperature distribution between 25° N and 85° N as computed from data for the year 1963. We see from Fig. 2 that there is reasonably good agreement between T_2 from the model and T_2 from observations for the dates of April 15 and October 15. However, the computed temperature difference betwen equator and pole is too large in the winter and too small in the summer. These discrepancies may possibly be explained by the fact that we have kept K constant during the year. According to Adem (1962) we should have a larger value than $2 \times 10^6\,\mathrm{m}^2\,\mathrm{sec}^{-1}$ for K in the winter. We would

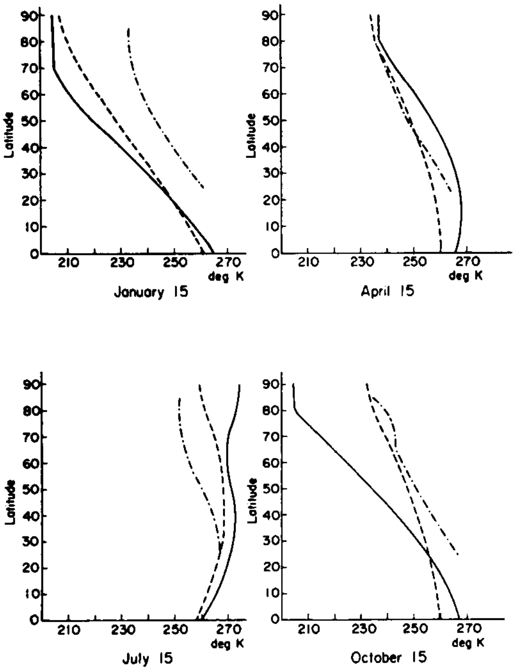

Fig. 2. The equilibrium temperature (*solid curve*), the computed temperature (*dashed curve*), and the observed temperature (*dashed-dotted curve*) as a function of latitude at four different times during a year.

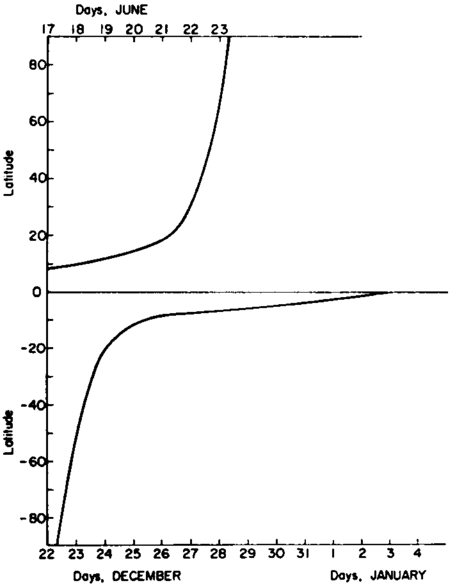

Fig. 3. The phase, measured in days, of the equilibrium temperature as a function of latitude. The upper scale applies to the Northern Hemisphere, the lower scale to the Southern Hemisphere.

consequently transport more heat from equator to pole and obtain a better agreement with observations. Similarly, the adopted constant value of K is too large during the summer as compared to Adem's data. Consequently, too much heat is transported from equator to pole resulting in a smaller temperature contrast than is observed. In spite of these differences our crude model is capable of describing several features of the annual variation of the zonally averaged temperature quite well. For example, the model predicts correctly that temperature in summer is larger at 30° N than at the equator. This reversed temperature gradient is evident in the cross section presented by Palmén & Newton (1967) (see Lorenz, 1967) for the time- and longitude-averaged temperature in July. Note also that the model is capable of creating a decrease in the temperature from 40° N to the pole, although the equilibrium temperature has a net increase in the same latitude belt.

We are next going to consider some phase relationships. Fig. 3 shows the time of maximum for the first harmonic of the annual variation of T_E. The upper time scale applies for the Northern Hemisphere while the lower time scale

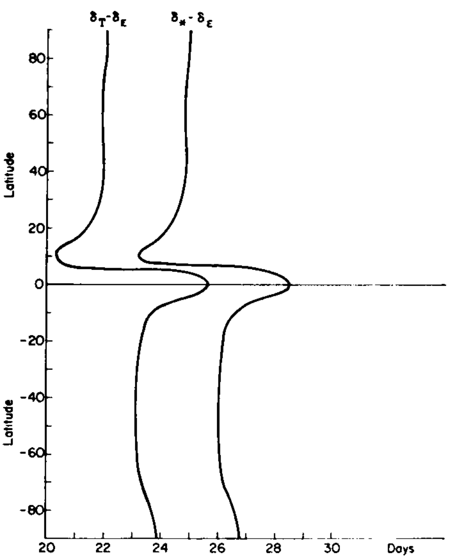

Fig. 4. The phase difference, measured in days, between the thermal stream function and the equilibrium stream function and between the vertical mean stream function and the equilibrium stream function as a function of latitude.

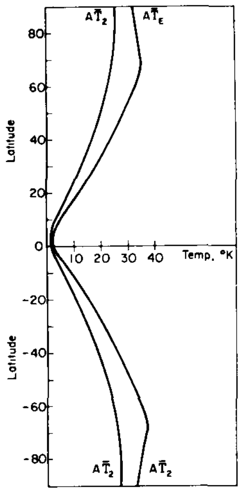

Fig. 5. The amplitudes of the first harmonic of the annual variation of the computed temperature, $\bar{T}_2$, and the equilibrium temperature, $\bar{T}_E$, as a function of latitude.

indicates the time of maximum for the Southern Hemisphere. The data used for the preparation of Fig. 3 can be obtained directly from a Fourier analysis at each latitude of the equilibrium temperature as it appears in Table 1. As expected we find a maximum temperature in the Northern Hemisphere around summer solstice. The variation in the time of maximum is only about 2 days between 20° N and 90° N. Similarly, the time of maximum equilibrium temperature in the Southern Hemisphere is around the summer solstice for that hemisphere, i.e., December 23. The variation of δ_E, the phase angle, is again only about 2 days between 90° S and 20° S, while a very rapid change takes place between 20° S and 20° N.

From the solution of the problem we may find the time of maximum for $\bar{\psi}_T$ and $\bar{\psi}_*$. The phase angle for $\bar{\psi}_T$ is the same as for $\bar{T}_2$ because of (3.1). Fig. 4 shows the differences $(\delta_T - \delta_E)$ and $(\delta_* - \delta_E)$ as a function of latitude from 90° S to 90° N measured in days. The difference $(\delta_T - \delta_E)$ is about 22 days in the latitude interval 20° N to 90° N and about 23 days from 90° S to 20° S. The typical time lag for $\bar{\psi}_*$, measured by $(\delta_* - \delta_E)$, is about 25 days and 26 days, respectively, in the same latitude regions. The rather large variations in δ_E, δ_T, and δ_* around the equator is of minor importance because the amplitude of the annual variation in this region is very small. This can be seen from Fig. 5 which shows the amplitudes, $A\bar{T}_E$ and $A\bar{T}_2$, of the first harmonic of the annual variations of $\bar{T}_E$ and $\bar{T}_2$ as a function of latitude. We notice that there is a reduction in amplitude at all latitudes, and that the amplitudes have a minimum at the equator.

We shall next consider the zonal winds as derived from the model. They are shown in Fig. 6 as a function of latitude for the upper level (25 cb) and the lower level (75 cb). For each level we have displayed the profile of the zonal wind for the annual mean and for the individual days, January 1 and July 1. It is seen that the winds are of the right order of magnitude as compared to similar diagrams for observed winds, Lorenz (1967). The winds are of larger magnitude at the upper level than at the lower level. There is a tendency to have a profile with two maxima especially in winter, but also in the annual mean. There are, however, several incorrect features of the computed zonal wind profiles as one would expect in view of the fact that the effects of the horizontal meridional transport of relative momentum have been neglected in the model. In addition to these factors, there may be other factors which are needed to obtain a more correct zonal wind-profile. It is for example likely that a more

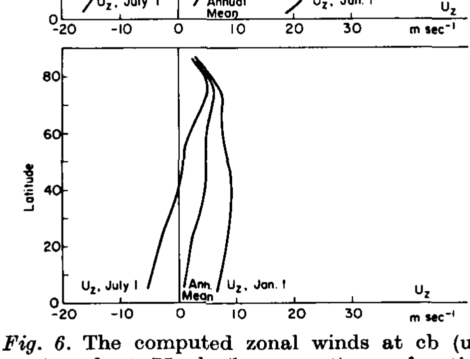

Fig. 6. The computed zonal winds at cb (upper part) and at 75 cb (lower part) as a function of latitude for the annual mean, January 1 and July 1.

realistic model than a quasi-geostrophic model is needed to explain the observed wind distribution in the tropics, where the profiles, computed here, are incorrect. The main discrepancy between the computed and observed wind profiles in the low latitudes is the failure to produce easterlies in the winter profile and the annual mean profile in the computed profiles. There is also a tendency to locate the wind maximum at too high a latitude in the computed profiles as compared to observed profiles.

The main idea in starting this investigation was to see if it was possible to reproduce from a theoretical model the major aspects of the observed annual variation of the energetics of the atmosphere. Observational studies show, as mentioned earlier, that the maximum amounts of available potential and kinetic energy are found in mid-January when energy calculations are carried out for the Northern Hemisphere north of 20° N. Estimates, based on the same calculations, show also that the maximum generation of available potential energy occurs around December 20, while the maximum conversion of available potential energy to kinetic energy takes place about January 8. The maximum dissipation of kinetic energy is found on January 17. No great emphasis should be attached to the specific dates. They were obtained from data for specific years, but there are indications (Kung & Soong, 1969) that there is not a very great variation when similar calculations are carried out based on other data samples. The main features are that the maxima for the amounts of energy occur in mid-January, and that there is about one month difference between the maximum generation of available potential energy and the maximum dissipation of kinetic energy.

We shall next investigate how well we are able to reproduce these features from the theoretical calculation. Using the parameters described earlier in this section, we have calculated the energy parameters given in eqs. (5.1) to (5.8). The results are best described by reproducing them in tabular form. Such a table is given as Table 3.

The values given in Table 3 may be compared with some of the values obtained in observational studies. The zonal available potential energy A_Z has been computed to be 3923 (1960), 3887 (1961), 4010 (1962). 2915 (1962), and 3164 (1963), where each value is expressed in kjm^{-2},

Table 3. *Annual mean values, amplitude, and phase of the first harmonic of the annual variation of various energy quantities computed with* $\varepsilon = 4 \times 10^{-6}$ sec^{-1}, $A = 0.6 \times 10^{-6}$ sec^{-1}, $\gamma = 0.4 \times 10^{-6}$ sec^{-1}, $K = 2 \times 10^6$ m^2 sec^{-1}, *and* $q^2 = 4 \times 10^{-12}$ m^{-2}

Units: kjm^{-2} for amounts of energy, kjm^{-2} sec^{-2} for remaining quantities

Energy quantity	Annual mean	Amplitude	Phase (days)
A_Z	3108	2042	14.2
K_{TZ}	134	73	14.3
K_{SZ}	538	293	17.2
K_Z	672	366	16.3
$G(A_Z)$	12.0×10^{-4}	8.8×10^{-4}	350.2
$D(K_Z)$	3.3×10^{-4}	1.8×10^{-4}	23.9
$C(A_Z, K_Z)$	3.3×10^{-4}	1.8×10^{-4}	0.3
$C(A_Z, A_E)$	8.7×10^{-4}	6.0×10^{-4}	17.1

and where the number in parentheses gives the year from which the data were taken (Wiin-Nielsen, 1967). Note that two values are given for the year 1962. The first value, 4010 kjm^{-2}, was based on data from two levels, 85 and 50 cb, while the second value was based on information from 8 pressure levels as was the value given for the year 1963. The last two values for 1962 and 1963 are therefore more correct, and our computed value (3108 kjm^{-2}) shows good agreement with the last two observed values of A_Z. Values of the amplitude of the first harmonic component for A_Z are: 1437 (1960), 1509 (1961), 1412 (1963), and 1196 (1963). Our computed value of 2042 kjm^{-2} is somewhat larger than the observed values. Finally, the values of the phase based on observations are: 16 (1960), 17 (1961), 17 (1962), and 20 (1963) as compared to our computed value of 14 days.

A similar comparison can be made for the zonal kinetic energy K_Z where the computed value is $K_Z = 672$ kjm^{-2} for the annual mean. Corresponding values based on observations are: 706 (1960), 679 (1961), 655 (1962), 779 (1962), and 832 kjm^{-2} (1963). The theoretical value of the amplitude is 366 kjm^{-2} while the observed values are 527 (1960), 499 (1961), 438 (1962), and 636 kjm^{-2} (1963). We observe that the theoretical value is somewhat smaller than the observed values. The phase of 16.3 days from the model compares with 20 days for the years 1960, 1961, and 1962, while the data from 1963 gave 24 days.

With respect to the amounts of energy we may therefore conclude that our model produces amounts which are of the correct order of magnitude, although we notice a tendency to get too large an amplitude in the annual variation for A_Z and too small an amplitude for K_Z. The phase computed from the theoretical model is essentially correct giving maximum energy values in mid-January.

An equally detailed comparison of the computed theoretical values for $G(A_Z)$, $C(A_Z, A_E)$, $C(A_Z, K_Z)$, and $D(K_Z)$ with values based on observations is not possible because these quantities are known with less accuracy. We note, however, that we obtain phase values which are essentially correct as compared to the data given by Wiin-Nielsen (1967), but also that our computed values of the annual mean values of $G(A_Z)$ and $C(A_Z, K_Z)$ appear to be somewhat smaller than values obtained from observational studies. This is especially true for $C(A_Z, A_E)$ where the observed values for the annual mean are: 27.1×10^{-4} (1960), 27.2×10^{-4} (1961), 29.0×10^{-4} (1962), and 23.7×10^{-4} kjm^{-2} sec^{-1} (1963) as compared to the theoretical value of only 12.0×10^{-4} kjm^{-2} sec^{-1}.

In summary, our theoretical model is partially successful in reproducing some of the major features of the atmospheric energetics and its annual variation. The best agreement with observational studies is obtained in the annual mean values of the amounts of energy and in reproducing phase values for the annual variation which are essentially correct. With respect to the amplitudes of the annual variations and the annual mean values of some of the energy conversions there is room for improvement.

7. Parameter studies

The values selected for the parameters ε, A, γ, K, and q^2 for the solution which has been described in detail in section 6 were obtained as the most likely values according to earlier studies. However, there is considerable uncertainty in several of the values and it is therefore of some interest to investigate how sensitive the solution is to our particular choice. Having five physical parameters at our disposal give us a large freedom in selection, and it is impossible to test all combinations. We shall therefore restrict ourselves to a few examples.

Table 4. *The upper part applies to* $\gamma = 0.8 \times 10^{-6}$ sec^{-1} *and the lower part to* $\gamma = 1.2 \times 10^{-6}$ sec^{-1}. $\varepsilon = 4.0 \times 10^{-6}$ sec^{-1}, $A = 0.6 \times 10^{-6}$ sec^{-1}, $K = 2.0 \times 10^6$ m^2 sec^{-1}, *and* $q^2 = 4 \times 10^{-12}$ m^{-2} *for both cases*
Table arranged as Table 3

γ	Energy quantity	Annual mean	Amplitude	Phase (days)
0.8×10^{-6}	A_Z	4846	3121	5.0
	K_{TZ}	213	111	5.1
	K_{SZ}	854	445	8.0
	$G(A_Z)$	16.5×10^{-4}	12.5×10^{-4}	338.5
	$D(K_Z)$	5.2×10^{-4}	2.7×10^{-4}	14.7
	$C(A_Z, K_Z)$	5.2×10^{-4}	2.8×10^{-4}	356.1
	$C(A_Z, A_E)$	11.3×10^{-4}	8.0×10^{-4}	8.3
1.2×10^{-6}	A_Z	5763	3650	1.1
	K_{TZ}	259	129	1.3
	K_{SZ}	1038	517	4.2
	$G(A_Z)$	16.1×10^{-4}	13.5×10^{-4}	331.9
	$D(K_Z)$	6.3×10^{-4}	3.1×10^{-4}	10.9
	$C(A_Z, K_Z)$	6.3×10^{-4}	3.2×10^{-4}	352.3
	$C(A_Z, A_E)$	9.8×10^{-4}	8.1×10^{-4}	5.0

We shall first test the solution with respect to the numerical value of γ, which had a value of 0.4×10^{-6} sec^{-1} in the case considered in section 6. Two new calculations with $\gamma = 0.8 \times 10^{-6}$ and $\gamma = 1.2 \times 10^{-6}$, but with the same values for all the other parameters were carried out. The results are given in Table 4. It is seen that the amounts of the various forms of energy increases when γ is increased. Some increase is also found in $G(A_Z)$, $C(A_Z, A_E)$, $C(A_Z, K_Z)$, and $D(K_Z)$, but these increases are not proportional to γ. With respect to the time of the maximum in the annual variation we find that the maximum occurs at an earlier time for all quantities when γ becomes larger, but the phase difference between $D(K_Z)$ and $G(A_Z)$ becomes larger with increasing values of γ being 38.7 days for $\gamma = 0.4 \times 10^{-6}$ sec^{-1}, 41.2 days for $\gamma = 0.8 \times 10^{-6}$ sec^{-1}, and 44.0 days for $\gamma = 1.2 \times 10^{-6}$ sec^{-1}. Of these values the first agree best with observations.

The numerical value of K is also quite uncertain. A number of numerical experiments were carried out to test the sensitivity of the solution to the value of K. The values of the other parameters were: $\varepsilon = 4.0 \times 10^6$ sec^1, $A = 0.6 \times 10^{-6}$ sec^{-1}, $\gamma = 0.4 \times 10^{-6}$ sec^{-1}, and $q^2 = 4 \times 10^{-12}$ m^{-2}. The numerical values of K were 0.5×10^6, 1.0×10^6, ..., 4.0×10^6 m^2 sec^{-1}. The results of this experiment are illustrated in the following figures.

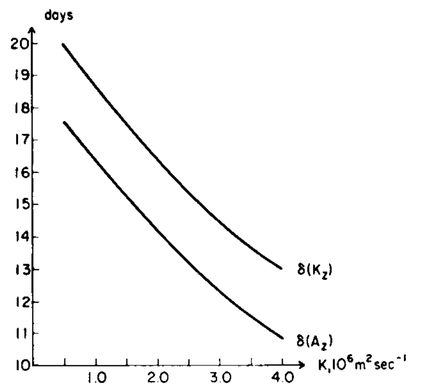

Fig. 7. The phase, measured in days, of the zonal available potential energy, A_Z, as a function of the diffusion coefficient, K, for heat.

Fig. 7 shows the phase of K_Z, $\delta(K_Z)$, and the phase of A_Z, $\delta(A_Z)$, given in days as a function of K. It is seen that the two curves are parallel indicating the phase difference between A_Z and K_Z is independent of the value of the diffusion coefficient for heat.

The other important phase relationships for $G(A_Z)$, $C(A_Z, A_E)$, $C(A_Z, K_Z)$, and $D(K_Z)$ are shown in Fig. 8 as a function of K. Two of these, the phase for $C(A_Z, K_Z)$ and $D(K_Z)$, change relatively little for increasing values of the diffusion coefficient K. This is perhaps to be expected because K influences first of all $C(A_Z, A_E)$ as seen from Fig. 8 and apparently also $G(A_Z)$. Fig. 8 shows that the phase difference between $G(A_Z)$ and $D(K_Z)$ changes relatively little for values of K larger than $2 \times 10^6 \, m^2 \, sec^{-1}$. However, if K were considerably smaller than this value the phase difference will be much larger than the value given in our example in the preceding section.

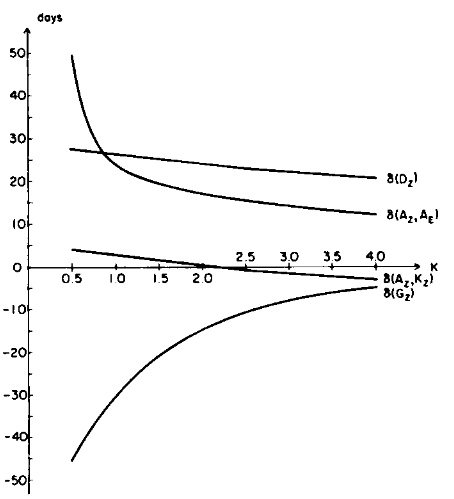

Fig. 8. The phase, measured in days, of the generation of zonal available potential energy, $G(A)_Z$, the energy conversion $C(A_Z, A_E)$, the energy conversion $C(A_Z, K_Z)$, and the dissipation of zonal kinetic energy $D(K_Z)$ as a function of the diffusion coefficient for heat.

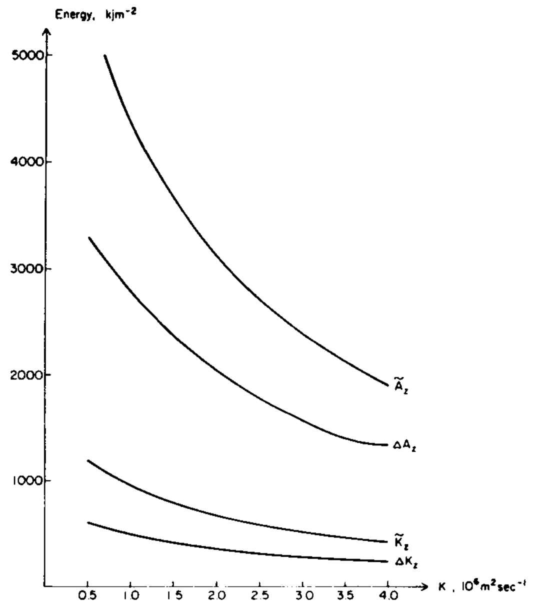

Fig. 9. The annual mean values of A_Z and K_Z and the amplitudes of the first harmonic of the annual variation of A_Z and K_Z as a function of the diffusion coefficient for heat.

Fig. 9 shows the annual mean values of the available potential energy, $\tilde{A}_Z$, and the kinetic energy, K_Z, together with the amplitudes of the first harmonics, ΔA_Z and ΔK_Z, as a function of the diffusion coefficient K. All of these quantities decrease with increasing K. Values of K much smaller than $2 \times 10^6 \, m^2 \, sec^{-1}$ will result in energy amounts which are larger than the observed amounts. We noticed in section 6 that $\tilde{A}_Z$ and $\tilde{K}_Z$ were approximately correct while ΔA_Z was too large and ΔK_Z too small. It is seen from Fig. 9 that this discrepancy cannot be corrected by simply changing the value of K.

The next figure, Fig. 10, shows $\tilde{G}(A_Z)$, $\tilde{C}(A_Z, A_E)$, and $\tilde{C}(A_Z, K_Z) = \tilde{D}(K_Z)$ as a function of K. It is apparent from this figure that if we are to obtain realistic values of $\tilde{G}(A_Z)$ and $\tilde{C}(A_Z, A_E)$ from the model we must select values

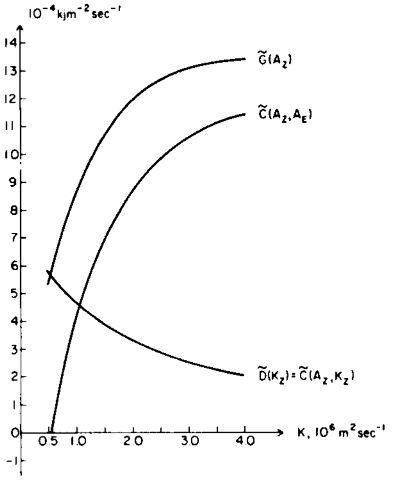

Fig. 10. The annual mean values of $G(A_Z)$, $C(A_Z, K_Z)$ as a funtion of the diffusion coefficient for heat.

of K which are at least as large as the one selected in the example given in section 6. Secondly, it is only when K is reasonably large that the results become less sensitive to the choice of K.

Fig. 11 shows the amplitudes of the first harmonic of $G(A_Z)$, $D(K_Z)$, $C(A_Z, K_Z)$, and $C(A_Z, A_E)$ as a function of K. It is apparent that these quantities vary in much the same way as the curves given in Fig. 10.

It is naturally possible to make a large number of additional numerical experiments with

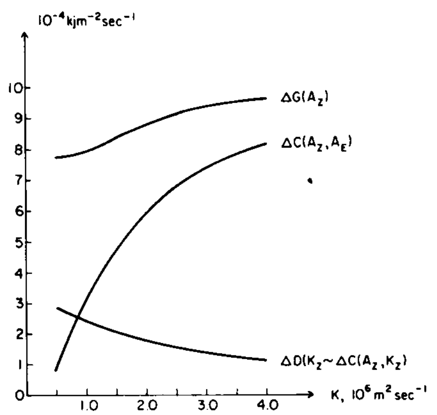

Fig. 11. The amplitudes of the first harmonic of the annual variation of $G(A_Z)$, $C(A_Z, A_E)$, $C(A_Z, K_Z)$, and $D(K_Z)$ as a funtion of the diffusion coefficient for heat.

the physical parameters. However, it is felt that the experiments described above illustrate the major properties of the model and that they concentrate on those parameters which are known with the smallest amount of accuracy.

8. Concluding remarks

A two-level, quasi-geostrophic model including a simple Newtonian form of diabatic heating and internal as well as boundary layer friction has been used to investigate certain aspects of the energetics of the atmosphere. The major additional assumptions which have been made in the study are that the meridional transport of sensible heat can be modeled by a diffusion approximation, and that the meridional transport of zonal relative momentum can be neglected in the first approximation. The latter approximation is best justified when the investigation is restricted to the largest meridional scale.

Under these assumptions it is possible to solve the zonally averaged equations of the model for the zonal average of the two stream functions which describe the flow and the temperature field. In addition to the zonal winds at the upper and lower levels of the model and the temperature field at the mid-level, it is possible to calculate the annual average and the first harmonic of the annual variation of the zonal available potential energy, the zonal kinetic energy, the generation of zonal available potential energy, the energy conversions from zonal available potential energy to eddy available potential energy and to zonal kinetic energy, and, finally, the dissipation of zonal kinetic energy.

It is found that the model is capable of rereproducing amounts of energy which compare favorably with observational studies as far as the annual mean is concerned. The annual variation of zonal available potential energy is somewhat larger than values indicated by observational studies, while the amplitude of the first harmonic of zonal kinetic energy is smaller than observed values. The phase relationships between the generation of zonal available potential energy, the conversion from this form of energy to zonal kinetic energy, and the dissipation of zonal kinetic is reproduced fairly well by the model, but there are some differences between the theoretical and the observed values for both the annual means and the amplitudes of the first harmonic of the annual variation, especially for the generation of the zonal available potential energy.

The major shortcoming of the present model apart from the fact that it is a two-level, quasigeostrophic model is probably the simplicity of the diabatic Newtonian heating and the neglect of the meridional transport of the zonal relative momentum. The diabatic heating effects can probably be modeled in a more realistic way, but it is more difficult to remove the other deficiency. However, the ideas presented by Saltzman & Vernekar (1968) and Green (1968) should be explored. A diagnostic study of the parameterization of momentum transport is presently underway.

9. Acknowledgments

The author is thankful to Mr. Perry Fisher and Mr. James Pfaendtner for the excellent help in programming all the calculations in this study.

REFERENCES

Adem, J. 1962. On the theory of the general circulation of the atmosphere. *Tellus 14*, 102–115.

Green, J. S. A. 1968. Transfer of heat and momentum by cyclone scale eddies in the general circulation. *Proceedings from the International Symposium on Numerical Weather Prediction, Tokyo, Japan, November 1968* IV, 17–20.

Krueger, A. F., Winston, J. S. & Haines, D. A. 1965. Computations of atmospheric energy and its transformation for the northern hemisphere for a recent five-year Period. *Monthly Weather Review 93*, 227–238.

Kung, E. C. & Soong, S. T. 1969. The march of seasons in kinetic energy of the atmosphere. *Quarterly Journal of the Royal Meteorological Society 95*, 501–512.

Lorenz, E. N. 1967. The nature of theory of the general circulation of the atmosphere. *World Meteorological Organisation* (Monograph), 161 pp.

Palmén, E. 1955. On the mean meridional circula tion in low latitudes of the Northern Hemisphere in winter and the associated meridional and vertical flux of angular momentum. *Societas Scientiarum Fennica, Commentationes Physico-Mathematicae 17*, 1–13.

Palmén, E. & Newton, C. 1967. *Atmospheric circulation systems*. Academic Press New York (in press).

Phillips, N. A. 1956. The circulation of the atmosphere: a numerical experiment. *Quarterly Journal of the Royal Meteorological Society 82*, 123–164.

Riehl, H. 1951. The North–East Trade of the Pacific Ocean. *Quarterly Journal of the Royal Meteorological Society*, *77*, 598–626.

Saltzman, B. 1968. Steady state solutions for the axially-symetric climatic variables. *Pure and Applied Geophysics 69*, 237–259.

Saltzman, B. & Vernekar, A. 1968. A parameterization of the large-scale transient eddy flux of relative angular momentum. *Monthly Weather Review 96*, 854–857.

Smithsonian Meteorological Tables. 1951. Sixth revised edition. Smithsonian Institute, Washington, D. C., 527 pp.

Wiin-Nielsen, A. 1962. On transformation of kinetic energy between the vertical shear flow and the vertical mean flow in the atmosphere. *Monthly Weather Review 90*, 311–323.

Wiin-Nielsen, A. 1967. On the annual variation and spectral distribution of atmospheric energy. *Tellus 19*, 540–559.

Wiin-Nielsen, A. 1968. On atmospheric response to large-scale seasonal forcing. *Proceedings from the International Symposium on Numerical Weather Prediction, Tokyo, Japan, November 1968* VI, 21–28.

Wiin-Nielsen, A., Vernekar, A. & Yang, C. H. 1967. On the development of baroclinic waves influenced by heating and friction. *Pure and Applied Geophysics 68*, 131-161.

ТЕОРЕТИЧЕСКОЕ ИЗУЧЕНИЕ ГОДОВОЙ ИЗМЕНЧИВОСТИ АТМОСФЕРНОЙ ЭНЕРГЕТИКИ

Используется зонально осредненные уравнения двухуровенной квазигеострофической модели для вычисления средних годовых значений и первой гармоники годового изменения температуры в средней тропосфере и зонального ветра на верхнем и нижнем уровнях. Неадиабатическое нагревание в модели принято в простейшей ньютоновской форме. Эффекты поверхностного и внутреннего трения включены вместе с простейшей параметризацией меридионального турбулентного переноса тепла в то время, как турбулентным переносом зонального относительного количества движения пренебрегается, ограничивая тем самым движение наибольшим меридиональным масштабом. Из решения этих уравнений можно получить средние годовые величины и первую гармонику годового изменения зональной доступной потенциальной энергии, зональной кинетической энергии, генерации зональной доступной потенциальной энергии, преобразования из этой формы в вихревую и затем в зональную кинетическую энергию, диссипации зональной кинетической энергии за счет трения.

Результаты показывают, что эта упрощенная форма способна воспроизводить важные аспекты атмосферной энергетики. Хорошо воспроизводятся фазовые соотношения, в том числе, сдвиг по времени между образованием зональной доступной потенциальной энергии и диссипацией кинетической энергии, так же как сдвиг между сезонным возбуждением и максимумами зональной доступной потенциальной и зональной кинетической энергии. Имеется разница между теоретическими результатами и наблюдениями в отношении интенсивности общей циркуляции и количеств энергии.